

# Polymaleamide–Polymaleimide Networks

D. Ivanov, C. Găină, C. Grigoraș

“P. Poni” Institute of Macromolecular Chemistry, Gr. Ghica Voda Alley 41A, 6600 Iasi, Romania

Received 5 February 2002; accepted 30 April 2003

**ABSTRACT:** Polymaleamide–polymaleimide networks were obtained as films by the thermal treatment of mixtures with different ratios of an aliphatic–aromatic polymaleamide (PMA) and 4,4′-bis(maleimidodiphenylmethane) (BMI), in *N*-methyl-2-pyrrolidinone (NMP) as a solvent. The polymaleamides were synthesized by ring-opening polyaddition of 1,6-hexamethylene–bisisomaleimide with 4,4′-diaminodiphenylmethane in NMP at room temperature. The networks are infusible and insoluble in organic solvents; therefore, they were studied by solid-state techniques such as IR, DSC, thermo-optical analysis (TOA), TG/DTG analysis, and TEM. Thermal treatment of pure PMA and BMI occurs with the

formation of crosslinked structures as proved by IR spectra. DSC and TOA curves show the appearance of chemical interactions between PMA and BMI in cured films and the formation of ordered morphologies, especially when BMI is the major component. TG/DTG and TEM results supported these observations. The PMA–polymaleimide network films present electrical insulator properties superior to individual polyamides or polyimides. © 2003 Wiley Periodicals, Inc. *J Appl Polym Sci* 91: 779–788, 2004

**Key words:** networks; crosslinking; morphology

## INTRODUCTION

The physical properties and processing characteristics of homopolymers are rarely favorable for practical the requirements needed for their use. Properties can be improved by combining the qualities of different polymers and are strongly related to the mixing degree of the components. It is quite difficult to mix polymers at a desired molecular level by blending or by separation from solution in mutual solvents (especially for those polymers that present limited miscibility).<sup>1</sup>

These problems can be avoided if networks of different polymers are formed. Thermal treatment (curing) is used to obtain networks with special thermal and electrical properties by simultaneous polymerization and crosslinking reactions that occur in monomer/polymer mixtures.<sup>2–4</sup>

Polymaleamides, which are polyamides with double bonds between the amide groups, offer the main advantage that no volatile products are evolved during the curing process as long as only addition reactions take place. Otherwise, the volatile compounds, if present, would produce voids in the material, thus causing deterioration, especially of the mechanical properties.<sup>5</sup> Addition reactions in polymaleamides lead to structures that contain polyamide units. The properties of polyamides are related to the type of substituents (aliphatic or aromatic) between the amide groups of the macromolecular chain. Polyamides with aliphatic soft segments are flexible chain polymers and

present low thermal expansivity, electrical insulation, and good adhesion properties. Aliphatic–aromatic polyamides combine the flexibility of aliphatic moieties with the high melt and glass transition temperatures induced by aromatic units.<sup>6</sup> The amide groups can lead, by hydrogen bonds, to polyamide self-associated structures; therefore, their density in the chain influences their properties.<sup>7</sup>

Polyimides exhibit high-temperature stability, excellent electrical properties, and mechanical strength. Polymaleimide resins are industrially important for composite materials and electronics-related products.<sup>8</sup>

This article presents the synthesis and characterization of some networks obtained by curing mixtures of aliphatic–aromatic polymaleamide (PMA) and 4,4′-bis(maleimidodiphenylmethane) (BMI) in different ratios. Both chain elongation and crosslinking reactions occur during thermal treatment. The chemical structure, morphology, and properties of the resulting networks depend on the initial BMI content in the mixtures.

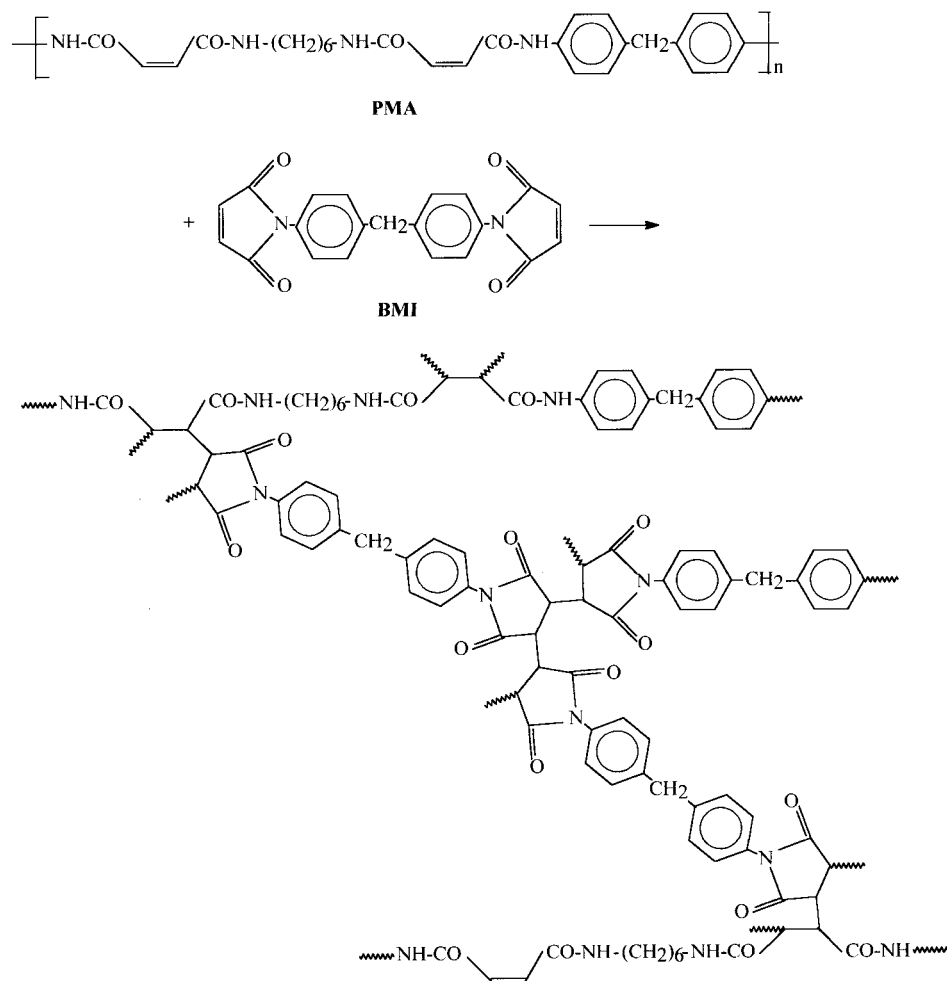
## EXPERIMENTAL

### Reagents and solvents

Maleic anhydride was purified (mp 56°C) by sublimation. 1,6-Diaminohexane (Fluka) was purified by vacuum distillation to give white crystals. 4,4′-Diaminodiphenylmethane was purified by recrystallization from benzene. The *N,N*′-dicyclohexylcarbodiimide (DCC) (Fluka) reagent was used as received. BMI (with the structure presented in Scheme 1) was prepared as described elsewhere<sup>9</sup> (mp 155–158°C).

*N*-Methyl-2-pyrrolidinone (NMP), dichloromethane, and *N,N*′-dimethylformamide were dried over P<sub>2</sub>O<sub>5</sub>

Correspondence to: D. Ivanov (dani@icmpp.tuiasi.ro).



**Scheme 1** Network synthesis by thermal crosslinking of initial components (PMA and BMI).

and fractionally distilled (bp 202–204, 40, and 153°C, respectively). Sulfuric acid, 98%, was a commercial product (Riedel-de Haën, Germany) and used without further purification.

### Preparation of PMA

An aliphatic–aromatic PMA was synthesized by ring-opening polyaddition (ROPA)<sup>10</sup> of 1,6-hexamethylene–bis(isomaleimide) (HBIM) with 4,4′-diaminodiphenylmethane, in an equimolar ratio, in NMP at room temperature, as elsewhere presented.<sup>11</sup> HBIM was obtained by cyclodehydration of the 1,6-hexamethylenebismaleamic acid using DCC as a dehydration agent.

#### 1,6-hexamethylenebismaleamic acid synthesis

A solution of 11.6 g (0.1 mol) of 1,6-diaminohexane in 70 mL glacial acetic acid was stirred during a dropwise addition of a solution of 19.6 g (0.2 mol) maleic anhydride in 50 mL of the same solvent. Stirring was

continued for 10 h. Bismaleamic acid that had precipitated during the reaction was removed by filtration, washed with water and with a 3% sodium carbonate solution, and dried under reduced pressure, at 60°C, for 6 h. Yield: 87%; mp 175°C.

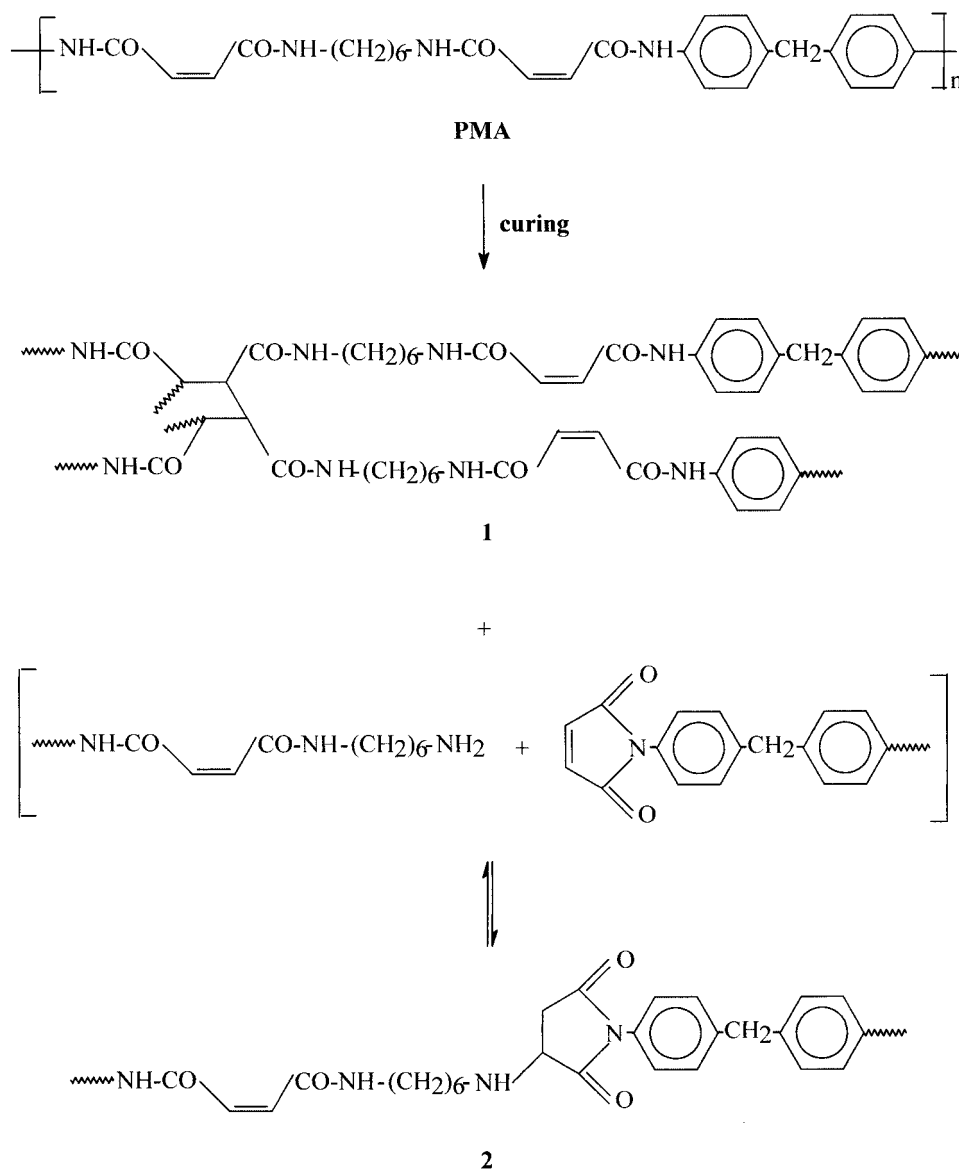
#### HBIM synthesis

The product was prepared by a dehydration reaction of 1,6-hexamethylenebismaleamic acid with DCC as described by Cotter et al.<sup>12</sup> Purification was performed by recrystallization from benzene: an ether mixture yielded a 65 wt % product with a melting point of 95–96°C.

IR (KBr)  $\text{cm}^{-1}$ : 1810–1790 (five-membered imide ring); 1695 ( $>\text{C}=\text{N}$ ).  $^1\text{H-NMR}$  (JEOL C-80 HL spectrometer,  $\text{CDCl}_3$ )  $\delta$ , ppm: 6.50–7.10 (two doublets, heterocycle vinyl  $\text{CH}=\text{CH}$ ).

#### PMA synthesis

A 6 g (0.03 mol) amount of 4,4′-diaminodiphenylmethane was added under stirring to a slurry of 8.3 g



Scheme 2 Possible reactions during PMA curing.

(0.03 mol) 1,6-hexamethylenebis(iso)maleimide in 12 mL NMP, and the reaction mixture was stirred for 5 h. The product was added to 50 mL distilled water when a sticky layer separated. After methanol solubilization, the product (with the structure depicted in Scheme 2) was precipitated in distilled water, removed by filtration, and washed with distilled water (with the structure as depicted in Scheme 2). Yield: 90%. Solubilization was realized in amide-type (NMP, etc.) solvents with 4% LiCl on heating. The inherent viscosity (measured at a concentration of 0.2 g/dL in NMP with 4% LiCl at 20°C using an Ubbelohde suspended level viscometer),  $\eta_{inh}$ , dL/g was 0.291. The polymer was freely soluble in 98%  $\text{H}_2\text{SO}_4$  but partially soluble in usual organic solvents.

IR (KBr)  $\text{cm}^{-1}$ : 3300 (N—H); 1640 (C=O, amide I); 1610 (C=C); 1550 (C—N, amide II).

The absence of the absorption band in the 980–960  $\text{cm}^{-1}$  region corresponding to the *trans* configuration also suggests that ROPA retained the *cis* geometry of the isomaleimide monomer, as was also mentioned in the literature.<sup>13,14</sup>

$^1\text{H-NMR}$  ( $\text{DMSO-}d_6$ )  $\delta$ , ppm: 6.10 (singlet, vinyl CH=CH); 6.75–7.30 (two doublets, *p*-disubstituted aromatic protons); 8.50 (CO—NH— $\text{C}_6\text{H}_4$  amide proton); 11.20 (CO—NH— $\text{CH}_2$  amide proton).

#### PMA-polymaleimide films curing

Twenty percent solutions each of PMA and BMI in NMP were obtained at room temperature under magnetic stirring. Different amounts from the two solutions were mixed to form films of various composi-

**TABLE I**  
**Codes and Compositions of Cured Films (Ratios of**  
**Initial PMA and BMI Solutions and Their**  
**Percent BMI Content)**

Sample code	PMA/BMI (mL/mL)	BMI (%)
Cured PMA	10/0	0
A10	9/1	10
A20	8/2	20
A40	6/4	40
A60	4/6	60
A80	2/8	80
A90	1/9	90
Cured BMI	0/10	100

tions, as presented in Table I. For instance, the A10 sample was prepared by adding 1 mL of the BMI solution to 9 mL of the PMA solution under stirring. The mixture was poured over a 120°C heated glass plate and maintained at 150°C for 1 h in an air atmosphere of a preheated convection oven to evaporate

the solvent; then, the temperature was maintained for 2 h at 220°C for the final thermal treatment. The obtained film was removed after cooling in a bath of water. After drying at about 100°C under a vacuum to remove water, the cured film was kept for 24 h in methanol to eliminate the solvent (NMP), then finally dried in similar conditions. The same treatment was applied to all solutions containing either the initial components or their mixture in different ratios.

#### Characterization and analysis techniques

The polymeric network films presented insolubility even in 98% H<sub>2</sub>SO<sub>4</sub>; therefore, their characterization requires the use of solid-state techniques. The chemical structures of the cured films were assigned on the basis of IR spectra recorded on an M80 Carl Zeiss Jena Specord spectrophotometer using KBr pellets.

Thermal behavior of the films was determined by thermogravimetric/differential thermogravimetric (TG/DTG) data obtained on 50-mg samples at a heating

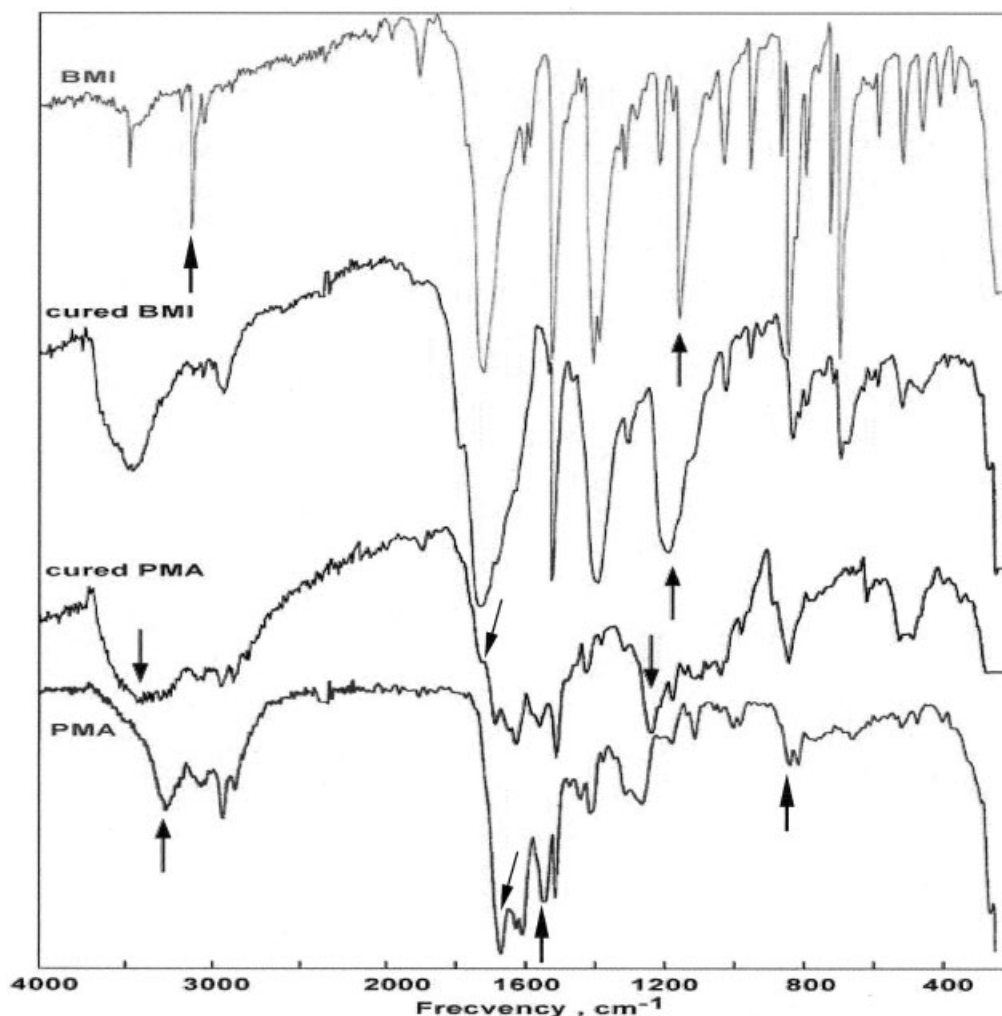


**Figure 1** IR spectra of the initial components (PMA and BMI) and their cured films.

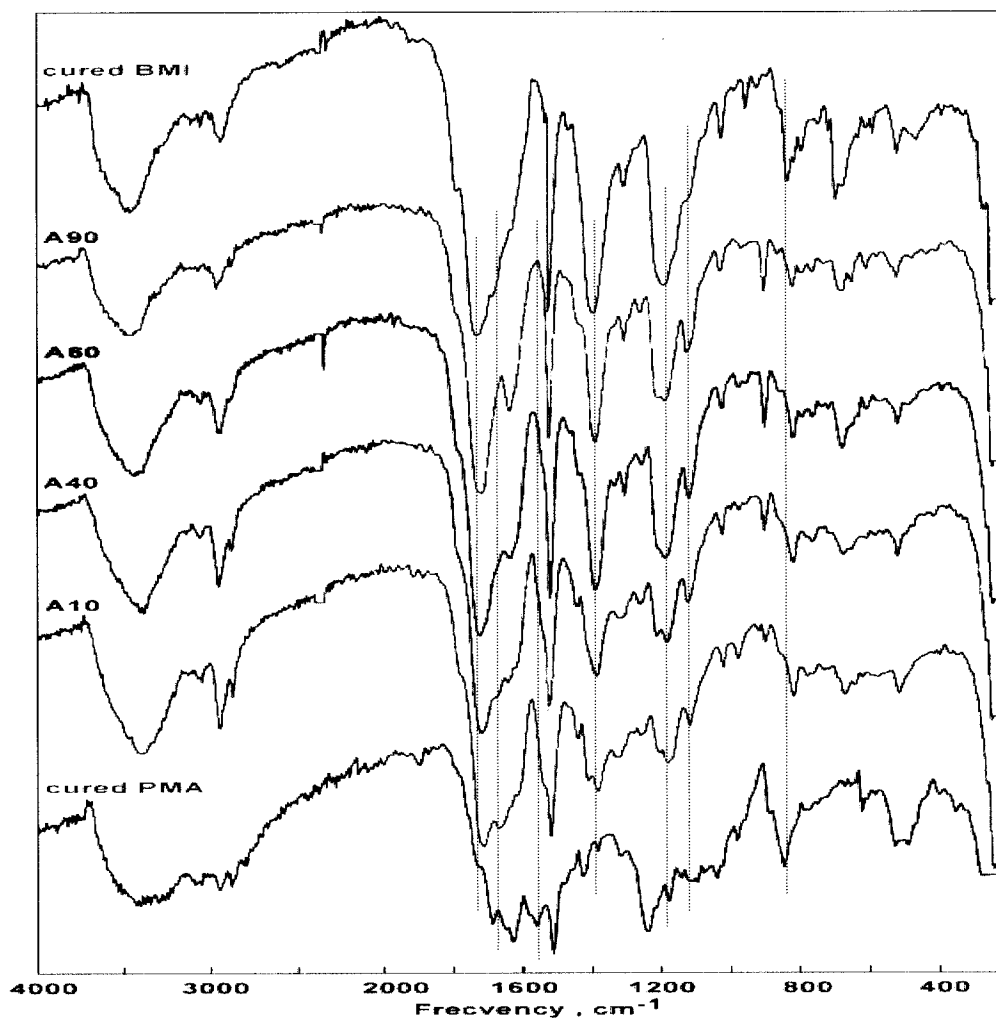


Figure 2 IR spectra of the cured components and network films.

rate of 12°C/min in air, using an MOM Budapest F. Paulik derivatograph. Differential scanning calorimetry (DSC) measurements were performed on a METTLER TA Instrument DSC 12E to determine the glass transition temperatures ( $T_g$ ) of the films and the thermal effects during curing of the initial components. The samples were heated in platinum crucibles in a 50 cm<sup>3</sup>/min N<sub>2</sub> flow at a 20°C/min heating rate. Thermo-optical analysis (TOA) was performed on an apparatus as described by Kovacs and Hobbs,<sup>15</sup> with a heating rate of 9.6°C/min. The thermo-optical transition temperature,  $T_{TOA}$ , was related to the inflexion point in the transmitted light intensity versus the temperature curve.

The morphology of the PMA-polymaleimide cured films was observed by transmission electron micrographs (TEMs) obtained on a Tesla BS513A microscope, using an ultrathin section technique performed on an ULTRAMICROTOM LKB-8001A apparatus, after araldite inclusions. The samples were initially

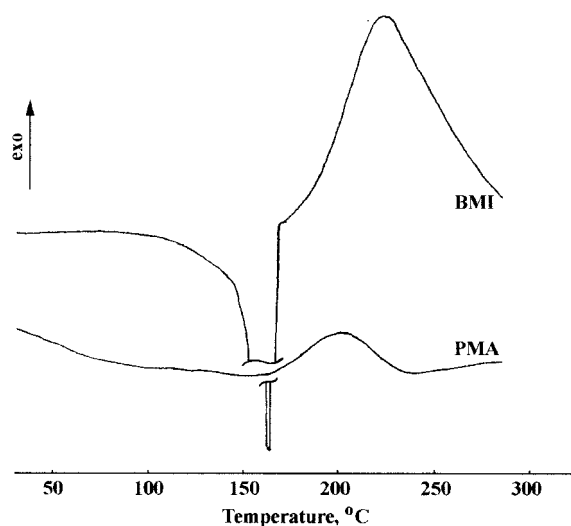


Figure 3 DSC curves for the initial components (PMA and BMI).

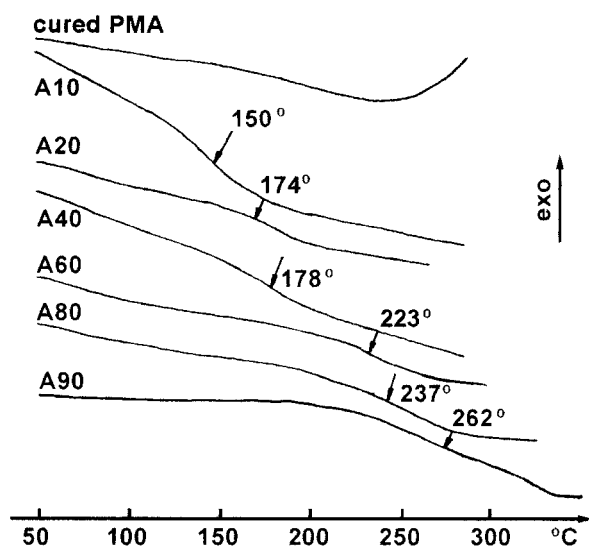


Figure 4 DSC curves for networks; glass transition temperatures ( $T_g$ ) are indicated by arrows; heating rate, 20°C/min.

treated with phosphowolframic acid, which induced a dark view for polyamide.

Electrical properties (volume resistivity and conductivity) of the cured films were performed on a digital RLC meter E0711. The volume resistivity was measured in direct current at 100 V using a TERALIN electrometer.

## RESULTS AND DISCUSSION

PMA is a hard-soft polymer that presents rigid malamide segments (due to extended conjugation between the amide groups and the unsaturated C=C bonds) and flexible  $-(CH_2)_6-$  aliphatic segments, both having similar length. The extended conjugation caused the  $\nu_{C=O}$  stretching vibration (amide I band) to appear in the IR spectrum at about 1675  $cm^{-1}$  (Fig. 1), corresponding to  $\alpha,\beta$ -unsaturated amide systems. The  $\delta_{NH}$  and  $\nu_{C-N}$  absorption bands (amide II, amide III) appear around 1550 and 1270  $cm^{-1}$ , respectively.<sup>16</sup> The  $\delta_{C=C}$  deformation vibration band in maleamide units appears around 830  $cm^{-1}$ . The amide dipolar structures (CO—NH) lead to interchain hydrogen bond formation; therefore, polyamides have the tendency to self-associate,<sup>17</sup> explaining their limited solubility. In PMA, this tendency is favored by the planar geometry of the maleamide conjugated segments. The  $\nu_{NH}$  vibration is presented as a distinct band about 3290  $cm^{-1}$ , characteristic for H bonds.

The IR spectrum of cured PMA presents larger peaks than for PMA, which can be due to partial crosslinking reactions during curing. The appearance of a new strong  $\nu_{C-C}$  band at about 1230  $cm^{-1}$  in the cured PMA spectrum proves the presence of a saturated branched structure<sup>18</sup> that resulted from

crosslinking between unsaturated bonds as depicted in structure 1 in Scheme 2. The amide I band at 1675  $cm^{-1}$  decreases in intensity and a shoulder appears at about 1720  $cm^{-1}$  that might correspond to the  $\nu_{C=O}$  stretching vibration in imide rings (maleimide or aspartimide). These structures could arise during curing by the breaking of the PMA chain, leading to maleimide and amine ends that can further undergo Michael addition (Scheme 2, structure 2).<sup>8</sup>

The evident displacement at higher frequency (3400  $cm^{-1}$ ) of the  $\nu_{NH}$  band in cured PMA could be explained by a lesser effect of the hydrogen bonds of the amide proton and a lower tendency to form self-associated structures. This might be due to the addition to the backbone of side chains that induces a lateral disorder and forces the chains apart. Therefore, IR observations suggest that a network might appear in cured PMA by crosslinking at former unsaturated groups. However, a partial unsaturation degree is still preserved, as shown by the 830- $cm^{-1}$  band.

The C=C double bonds in BMI are highly electron-deficient because of the two imide carbonyl groups on either side; therefore, they can easily undergo polymerization reactions during curing. BMI homopolymerization is supported in the IR spectrum of the cured film by the strong decrease of the 3100- $cm^{-1}$  band ( $\nu_{=CH}$ ) compared to the BMI spectrum and by the displacement of the bands at 1165  $cm^{-1}$  ( $\nu_{C-N-C}$  in maleimide) to about 1185  $cm^{-1}$  ( $\nu_{C-N-C}$  in succinimide).<sup>19</sup> The absorption bands also became broader in

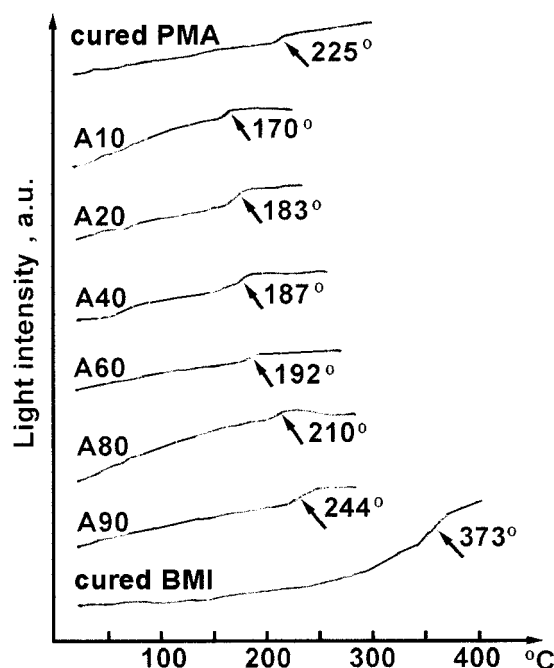


Figure 5 Transmitted light intensity versus temperature for cured films; arrows mark thermo-optical transition temperatures ( $T_{TOA}$ ); heating rate, 9.6°C/min.

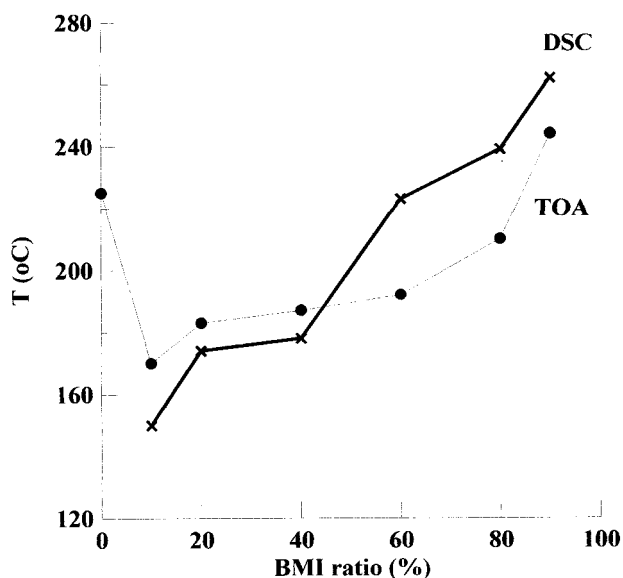


Figure 6 Transition temperatures ( $T_g$  and  $T_{TOA}$ ) evolution versus BMI ratio.

cured BMI, proving that the polymerization proceeds with a high tendency to form crosslinked networks.<sup>20</sup>

The films of various PMA/BMI compositions presented in Table I were obtained as previously described. In the IR spectra of the A10–A90 series films (Fig. 2), one can notice the bands corresponding to both cured BMI (1720, 1385, and 1185  $\text{cm}^{-1}$ —imide I, II, and III bands, respectively) and cured PMA (1680 and 1550  $\text{cm}^{-1}$ —amide I and II, respectively). As expected, the imide bands increase with the BMI content, and in the A80 sample, they cover the amide bands. It has to be mentioned that the decreasing intensity in the A10–A90 series of the  $\delta_{\text{C}=\text{C}}$  band at 840  $\text{cm}^{-1}$  from maleimide units indicates that saturation of the double bonds occurred. Moreover, the  $\nu_{\text{C}-\text{N}-\text{C}}$  absorption band at about 1165  $\text{cm}^{-1}$  from the maleimide units decreases in the A10 and A20 samples compared to the cured PMA and vanishes in the other samples. These remarks suggest that, in the A10 film, the double bonds in BMI could attack the vinyl groups in PMA, which explains the shoulder at 1165  $\text{cm}^{-1}$ . In further films in the series, BMI reacted either by homopolymerization or with PMA vinyl groups, which explains the decrease of the content in the maleimide groups (Scheme 1).

Brown and Sandreczki<sup>21</sup> proposed a detailed mechanism of thermal polymerization of the maleimide functions in BMI as a radical polyaddition. Based on electron paramagnetic resonance spectral data, they considered that homopolymerization involves, as thermal priming, the scission of a double bond, leading to a biradical. Subsequently, the biradical attacks another double bond with two additional radical supplies, one active and the other inactive. The active one

reacts as an intermediate in the formation and growth of a polymeric network.

The DSC curve for BMI presents a strong endotherm of melting with a minimum at 158°C, immediately followed by a large exotherm corresponding to polymerization, as reported in the literature (Fig. 3).<sup>8</sup> For PMA, the DSC curve shows an exotherm with a maximum at about 200°C, which corresponds to the double-bond reaction. The process starts in the same temperature range as that of BMI melting. In PMA/BMI mixtures, one can expect the polymerization of the two components to take place simultaneously. Reaction conditions also permit the radical transfer between BMI and PMA double bonds, which could lead to PMA–polymaleimide network formation (Scheme 1).

For cured PMA, the DSC curve corresponds to a rigid structure and it is practically difficult to establish a  $T_g$  value that might be close to the initial temperature of degradation (Fig. 4). When 10% BMI is added (A10 sample), one inflexion point appears at 150°C, meaning that the newly formed structure could be a flexible one, even if benzene rings are included. This might be explained by the addition of BMI as side chains to the PMA backbone that took place with the interruption of the extended conjugation. Substituted saturated groups, having increased mobility, are formed that strongly decrease the self-association tendency. The monotone increase of  $T_g$  with the BMI amount in the A10–A90 series is due to both crosslink-

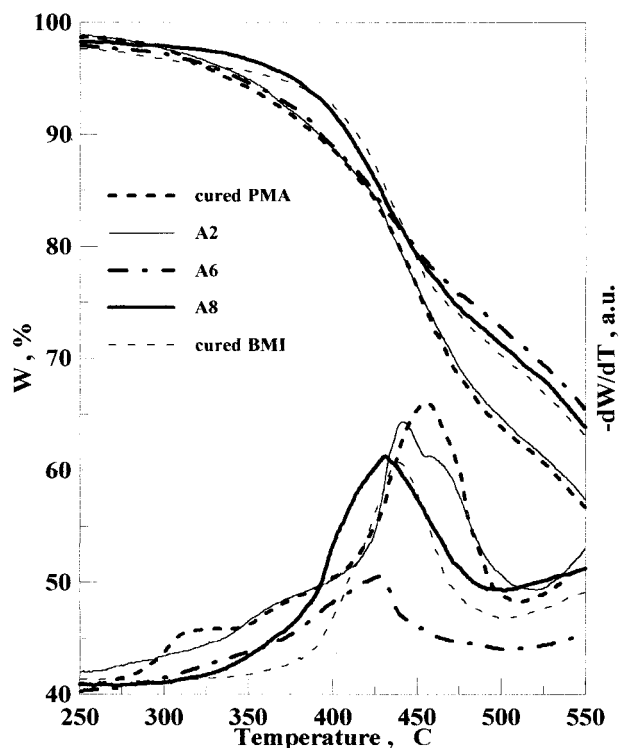
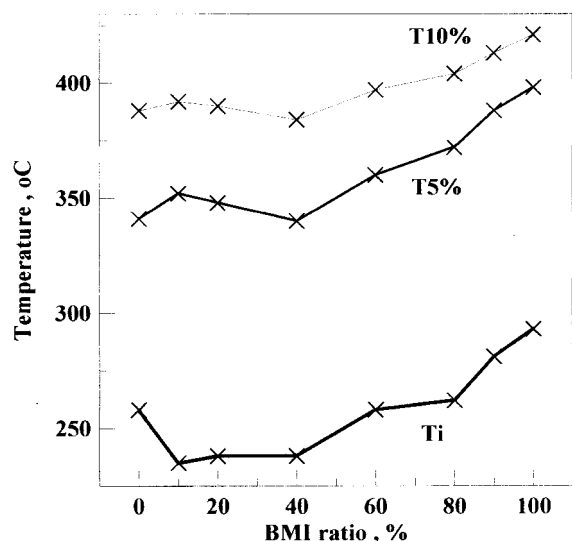


Figure 7 TG and DTG curves for cured films.



**Figure 8** Characteristic temperatures (initial temperature,  $T_i$ ; temperatures for 5 and 10% weight loss,  $T_{5\%}$  and  $T_{10\%}$ , respectively) for thermal decomposition of the cured films.

ing and BMI homopolymerization. The same effect was noticed for epoxy–novolac/bismaleimide networks.<sup>22</sup>

Thermal rigidization in the A10–A90 series was also confirmed using TOA analysis (Fig. 5) by the monotone increase of  $T_{TOA}$  with an increasing BMI amount. The TOA method allowed the determination of the transition temperature for both cured PMA (at 225°C) and cured BMI (at 373°C), which was not successful by DSC measurements. TOA also confirmed that the PMA/BMI cured films have a more flexible structure than that of both individually cured components, which might be explained only by the reactions between the components, as previously mentioned. For instance, the decrease of  $T_{TOA}$  at 55°C from cured PMA to A10 suggests the detachment of self-associated structures having high densities when a low amount of BMI is added. This could be explained by crosslinking reactions rather than by a physical mixture of the components. The great difference of 130°C in  $T_{TOA}$  between A90 and cured BMI could be due to the strong decrease of the crosslinking density when PMA is present.

Interesting conclusions were obtained when comparing  $T_{TOA}$  and  $T_g$  values (Fig. 6). DSC data through specific heat represent a measure of changes in the molecular mobility, while TOA data through a refractive index are a measure of changes in the material density (according to the Lorentz–Lorenz relation). Using similar analysis conditions as in present study, Schultz and Gendron<sup>23</sup> reported almost parallel curves for the dependence of  $T_{TOA}$  and  $T_g$  values on the resin composition for polystyrene/poly(propylene oxide) blends. For PMA/BMI mixtures, we observed slowly ascending and parallel curves for  $T_{TOA}$  and  $T_g$

with an increasing BMI content until the amounts of the components were equal. When BMI becomes the major component of the sample (A60),  $T_g$  suffers a significant increase in respect to  $T_{TOA}$ . Compared to the A40 sample, the A60 one corresponds to a structure with lower flexibility at a similar density, which can be explained by an increasing of the morphology order.

The TG and DTG curves of some cured films are presented in Figure 7. All the studied samples decompose without previous melting and with a 30–35% weight loss below 500°C in a single major step having distinct TG and DTG curves (Fig. 7). The relative low weight loss is not surprising if one considers the amount of heterocycles and aromatic rings in the structure.

The DTG curve of cured PMA shows a clear peak at about 410–510°C, preceded by a long slope in the 270–360°C temperature range, which corresponds to about a 10% weight loss. This value corresponds to ammonia formation<sup>6</sup> from amine ends resulting from the chain scission over an aliphatic amide group and by retro-Michael reactions. Cured BMI presents a higher thermal stability than that of cured PMA, evidenced by the lower final weight loss and the shift of the TG curve to higher temperatures despite the maximum of the decomposition rate that appears at 438°C compared to 455°C in cured PMA.

The A10 film has a similar thermal stability as that of cured PMA, except for the minor peak in the 270–360°C temperature range. This behavior could be explained by the Michael addition over the BMI maleimide of ammonia or amine that resulted during thermal scission of the PMA chains. The DTG curve shows a peak analogous to cured BMI and a shoulder corresponding to cured PMA, although the latter represented the major component. This suggests the appearance of interactions between components that favors the decomposition of the BMI units to the detriment of the PMA ones. For the samples from A10 to A60 (A20 and A40 not shown in Fig. 7), the initial moments of decomposition are similar to the ones of cured PMA but the final weight loss decreases, as expected from the increasing BMI content. The weight loss above 450°C of the A60 sample is smaller than that of the cured BMI; therefore, the BMI units are stabilized compared to other samples in the series, which supports the idea of a highly crosslinked structure. The decomposition of the A90 sample is similar to that of cured BMI; however, a lower thermal stability can be observed, especially for the initial moments of the process as an effect of crosslinks with PMA chains.

The characteristic temperatures (initial temperature,  $T_i$ , and temperatures for 5 and 10% weight loss,  $T_{5\%}$  and  $T_{10\%}$  respectively) for the thermal decomposition of the A10–A90 samples increase with the BMI content



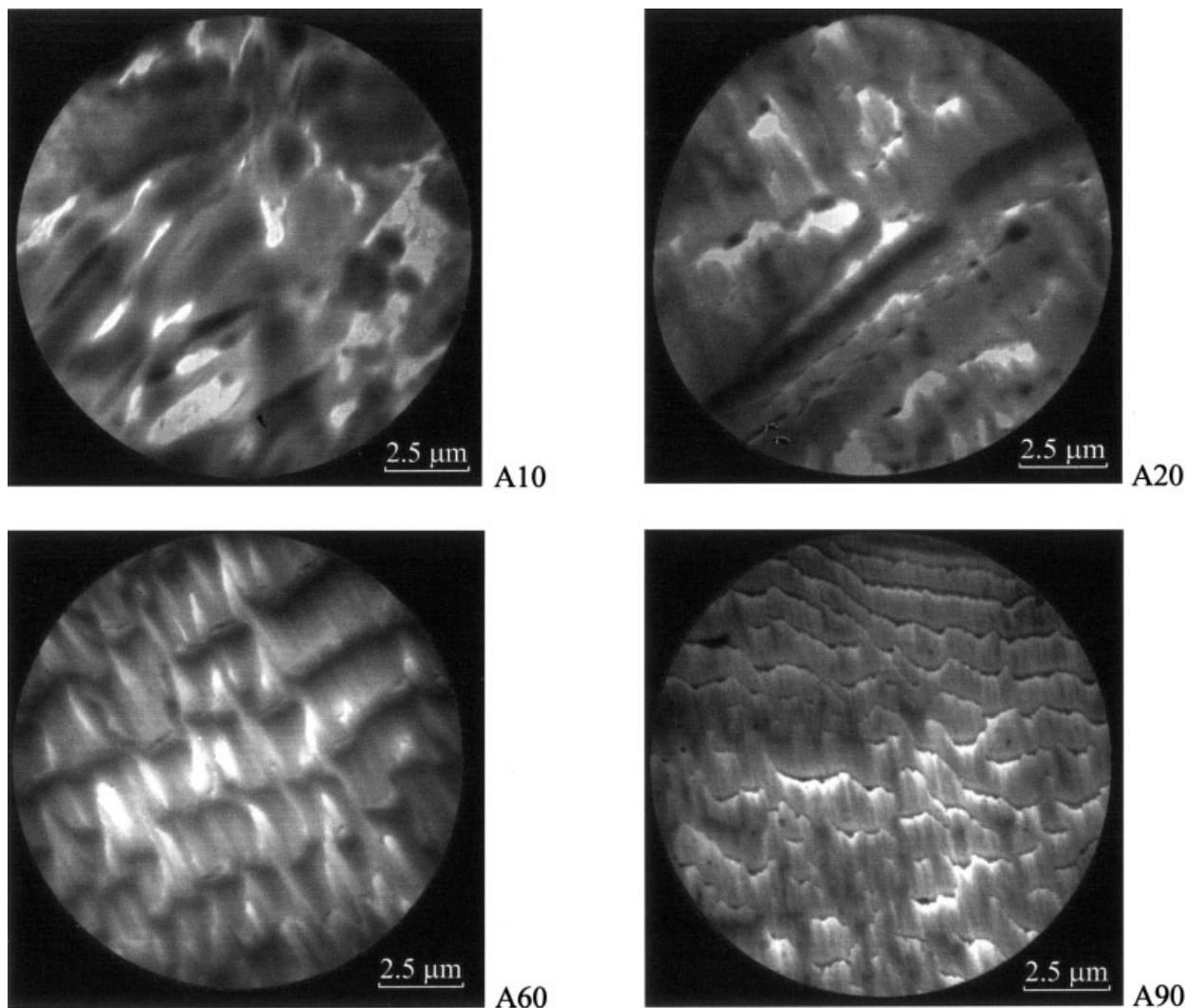


**Figure 9** TEMs of some films; the order in the network morphology increases with an increasing BMI ratio.

(Fig. 8), showing an increase of thermal stability. This behavior was also noticed for other BMI-containing networks.<sup>21</sup>

The morphology of the system was revealed from TEMs. The images were studied in planes of a section taken under different angles, providing the spatial order. Hence, if we consider the A10 film (Fig. 9), the dark zone corresponds to PMA, the light ones to BMI, and the majority homogeneous gray zones to a possible crosslinked PMA-polyimide structure; the white zones represent accidental voids. No clear separation border between PMA and BMI phases is seen, which can be explained by crosslinks rather than by an intimate mixing. In A20, the formation of an ordered net-type structure can be observed that is quite homogeneous but not compact. Beginning with A60 in the series, an ordered structure is proved. This was observed for images taken under different angles; therefore, the structure corresponds to a tridimensional developed network. The ordered network structure

becomes denser in A90, which contains the highest initial BMI amount. Morphological visualization confirms and explains the previous observations obtained from other analysis methods and together supports that crosslinking takes place during curing of the PMA/BMI mixtures.

The networks obtained as films were characterized by electrical measurements. The new structures present electrical insulator properties such as high-volume resistivity ( $2.15\text{--}7.92 \times 10^{16} \Omega \text{ cm}$ ) and low conductivity ( $1.26\text{--}4.65 \Omega^{-1} \text{ cm}^{-1}$ ). These values indicate superior properties compared to individual polyamides and polyimides.<sup>24</sup>

## CONCLUSIONS

PMA-polymaleimide networks were synthesized by thermal-treated mixtures of an aliphatic-aromatic PMA and 4,4'-BMI in different ratios. PMA was obtained by ROPA of 1,6-hexamethylene-bis(isomaleim-

ide with 4,4'-BMI in NMP, at room temperature. The networks were obtained as insoluble films; therefore, solid-state techniques were used for their characterization. Curing of single PMA and BMI occurred with formation of crosslinked structures as proved by IR spectroscopy. DSC and TOA showed the appearance of interactions between PMA and BMI in mixtures and the formation of ordered morphologies, especially when BMI is major component. TG analysis and TEM supported these observations. The network films presented electrical insulator properties superior to individual polyamides and polyimides.

## References

1. Ree, B. M.; Yoon, Y. In *Interpenetrating Polymer Networks; Advances in Chemistry Series*; American Chemical Society: Washington, DC, 1994; Chapter 12.
2. Landis, A. L.; Lau, K. S. Y. U.S. Patent 4 996 101, 1991.
3. Luo, J.; Zhan, C.; Qin, J. *React Funct Polym* 2000, 44, 219.
4. Kumar, A. A.; Alagar, M.; Rao, R. M. V. G. K. *J Appl Polym Sci* 2001, 81, 38.
5. Viswanathan, S.; Nagarathinam, R.; Rajeswari, N. *Polymer* 1997, 38, 217.
6. Sweeny, W.; Zimmerman, J. In *Encyclopedia of Polymer Science and Technology*; Wiley-Interscience: New York, 1969; Vol. 10.
7. Alemain, A. C.; Puiggali, J. *Rec Res Dev Polym Sci* 1996, 1, 33.
8. Grenier-Loustalot, M.-F.; Da Cunha, L. *Polymer* 1997, 39, 1833.
9. Sava, M.; Chiriac, C.; Gaina, C.; Stoleriu, A.; Gaina, V. *J Macromol Sci Pure Appl Chem A* 1997, 34, 725.
10. Imai, Y.; Ueda, M.; Kanno, S. *J Polym Sci Polym Chem Ed* 1975, 13, 1691.
11. Ivanov, D.; Gaina, C. In *Proceedings of the International Conference on Materials Science and Engineering, BRAMAT 2003, Brasov, Romania, March 13–14, 2003; Vol. 4, p 187.*
12. Cotter, R. J.; Sauers, C. K.; Whelan, J. M. *J Org Chem* 1961, 26, 10.
13. Varma, I. K.; Veena, I. K. *J Polym Sci Polym Chem Ed* 1979, 17, 163.
14. Mortillera, L.; Russo, M.; Credali, L.; Guidotti, V. *Macromol Chem* 1969, 126, 239.
15. Kovacs, A. J.; Hobbs, S. Y. *J Appl Polym Sci* 1972, 16, 301.
16. Balaban, A. T.; Banciu, M.; Pogany, I. *Aplicatii ale metodelor fizice in chimia organica; Stiintifica si Enciclopedica: Bucuresti, 1983; Chapter 2.*
17. Challis, B. C.; Challis, J. A. In *Comprehensive Organic Chemistry*; Barton, D.; Ollis, W. D., Eds.; Pergamon: Oxford, 1979; Vol. 2, Chapter 9.
18. Avram, M.; Mateescu, Gh. D. In *Infrared Spectroscopy*; Tehnica: Bucuresti, 1966; Part III, Chapter 1.
19. Di Giulio, C.; Gautier, M.; Jasse, B. *J Appl Polym Sci* 1984, 29, 1771.
20. Hummel, D. O.; Heinen, K.-U.; Stenzenberger, H.; Siesler, H. *J Appl Polym Sci* 1974, 18, 2015.
21. Brown, I. M.; Sandreczki, T. C. *Macromolecules* 1990, 23, 94.
22. Vanaja, A.; Rao, R. M. V. G. K. *Eur Polym J* 2002, 38, 187.
23. Schultz, A. R.; Gendron, B. M. *J Appl Polym Sci* 1972, 16, 461.
24. Harper, C. A. In *Encyclopedia of Polymer Science and Technology*; Wiley-Interscience: New York, 1966; Vol. 5.